

Manipulating White-Light Generation in Adamantane-Like Molecules via Functional Group Substitution

Saravanan Gowrisankar^{+, [a]}, Christopher A. Hosier^{+, [b]}, Peter R. Schreiner,^{*, [a]} and Stefanie Dehnen^{*, [b]}

Certain adamantane (Ad)-like molecules, either clusters of the type $[(R'T)_4E_6]$ with inorganic cores (R' = cyclic/aromatic organic substituent; $T = \text{Si, Ge, Sn}$; $E = \text{S, Se, Te}$) or adamantane derivatives $[(R'C)_4(\text{CH}_2)_6] = \text{Ad}R'_4$, display extreme nonlinear optical properties, which can lead to white-light emission when exposed to near infrared light. While previous studies have established some requirements for these compounds to generate white light, the ability to tailor this effect remains elusive. Here we evaluate the impact of a variety of inorganic

and organic compounds with Ad-like cores as well as various functional groups on white-light generation (WLG). We show that polarization and electron density localization are influenced by the type of the functional group R in $[(R\text{-PhSn})_4S_6]$ in particular, according to DFT computations. While these groups do not have a large impact on the maximum emission wavelengths, they do significantly affect the laser power threshold for the occurrence of WLG.

Introduction

Generation of light in a controlled manner is fundamental to modern-day society. Light generation is a key aspect of materials used in a variety of applications such as analytical probes,^[1] chemical transformations,^[2] display screens,^[3] and *in vivo* imaging.^[4] Prime examples of the importance of such materials are light-emitting diodes (LEDs). The development of LEDs with different emission spectra led to the production of lightbulbs and electronic screens that are more energy efficient, have longer lifetimes, and have better color tunability relative to their predecessors.^[5]

We have recently reported the generation of highly directional white light with amorphous adamantane-like compounds of the type $[(R'Sn)_4S_6]$ (R' = aromatic/cyclic organic substituent) when exposed to a continuous near-infrared light source.^[6] To date, we have successfully demonstrated that all aspects of the cluster (i. e., the atoms present in the adamantane-like core and

the external substituents) can be substituted while retaining white-light generation (WLG) properties, allowing for engineering of these materials for potential directed light applications.^[6a,7] From these works, we determined several criteria that appear to be critical to the generation of white light: the compound must be obtained as an amorphous powder, it must have a sufficiently large HOMO-LUMO gap, and ligands must be sufficiently electron-rich. One challenge that remains, however, is the ability to fine tune the emission spectra produced by these compounds.^[7]

We hypothesized the emission spectrum could be modified by manipulating the electronic structure of the cluster using substituents with additional functional groups. Electron-donating and electron-withdrawing groups (EDGs and EWGs, respectively) are well-known to modify the HOMO-LUMO gaps of molecules, which can affect excitation properties. Substituents bearing additional functional groups were previously shown to influence nonlinear optical properties of other tin complexes.^[8] As such, functional groups could serve as a means for modulating the WLG properties of these compounds. For shedding light on these effects, we designed a comprehensive study covering a series of known inorganic-organic hybrid clusters of the type $[(R\text{-PhSn})_4S_6]$, based on the prototypic $\{\text{Sn}_4\text{S}_6\}$ cluster core, for which the WLG effect was observed for the first time, and their organic $[(R\text{-C}_6\text{H}_4)_4(\text{CH}_2)_6] = \text{Ad}(R\text{-Ph})_4$ analogs.

Results and Discussion

We began our investigation with quantum chemical studies.^[9] We employed density functional theory (DFT) methods and computed the natural population analysis (NPA) partial charges^[10] of the respective atoms in various related $[(R\text{-PhSn})_4S_6]$ and $\text{Ad}(R\text{-Ph})_4$ compounds. Functional groups were

[a] Dr. S. Gowrisankar,[†] Prof. Dr. P. R. Schreiner
Institute of Organic Chemistry and Center for Materials Research (ZfM/Lama)
Justus Liebig University
Heinrich-Buff-Ring 16, 35392 Giessen (Germany)
E-mail: prs@uni-giessen.de

[b] Dr. C. A. Hosier,[†] Prof. Dr. S. Dehnen
Fachbereich Chemie and Wissenschaftliches Zentrum für Materialwissenschaften (WZMW)
Philipps-Universität Marburg
Hans-Meerwein-Str. 4, 35043 Marburg (Germany)
E-mail: dehnen@chemie-uni-marburg.de

[†] These authors contributed equally to this work.

Supporting information for this article is available on the WWW under <https://doi.org/10.1002/cptc.202200128>

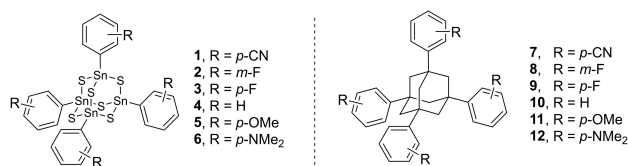
© 2022 The Authors. ChemPhotoChem published by Wiley-VCH GmbH. This is an open access article under the terms of the Creative Commons Attribution License, which permits use, distribution and reproduction in any medium, provided the original work is properly cited.

chosen to cover a range of Hammett σ values, with the hope of quantifying EDG or EWG effects (Scheme 1).^[11] Computations were performed using the def2-TZVP basis set^[12] with an effective core potential ECP-46 for the Sn atoms^[13] in conjunction with the PBE0 functional.^[14] The results are summarized in Table 1.

For the Sn/S-based clusters, the computations reveal a correlation between the charge separation in the molecule and the Hammett σ values. The presence of stronger EWGs results in a slight decrease of the negative partial charge at the S atoms and in an overall increased charge separation between the Sn–S core and the ligands. Conversely, the presence of EDGs leads to smaller charge separation between the core and ligands. By contrast, for the purely organic adamantane derivatives and the same set of substituents, the charge separation is substantially smaller between the adamantane core and the aryl groups, and functional group exchanges only have a small impact. We also performed time-dependent density functional theory (TD-DFT) computations to explore the effect of functional groups on the first singlet excitation in these compounds. The difference in electron densities obtained this way for the first singlet adiabatic excitation event are illustrated in Figure 1, along with the lowest singlet excitation energies.

In the case of [(R-PhSn)₄S₆], functional groups with larger positive Hammett σ values (i.e., EWGs, “acceptors”) results in density changes resembling a core-to-ligand excitation, whereas the presence of functional groups with larger negative Hammett σ values (i.e., EDGs, “donors”) result in electron density changes resembling a ligand-to-core excitation, which is intuitive.

Of particular note is the –NMe₂ group (the best electron donor in the series), which causes a substantial separation of excess density between the ground and excited states.



Scheme 1. Arylated adamantane-type clusters [(R-PhSn)₄S₆] (left) and adamantane derivatives Ad(R-Ph)₄ (right) with various functional groups.

The correlation with the computed lowest singlet excitation energies is not strict though: while this value smoothly increases as the Hammett σ values decreases for compounds 1–5, it drops when changing the functional group from –OMe (in 5) to –NMe₂ (in 6). This difference is consistent with the described difference electron density and with a smaller computed HOMO-LUMO gap relative to the other compounds. Obviously, the electron-pushing effect of the –NMe₂ groups is in a region, in which the excitation is greatly facilitated. Overall, these results confirm that for the inorganic adamantane-based clusters, functional groups notably affect the excitation event – with said limit being surmounted even for –OMe.

The correlation between the Hammett σ value and the excitation behavior is less obvious for Ad(R-Ph)₄. We observe a similar, yet overall weaker trend when going from 7 to 12 in the location of excess electron density. The computed excitation energies do not show a linear trend, but again it drops for –NMe₂ groups. This is likely a result of the electronic level energies of the core and the ligands being far closer than for mixed inorganic-organic clusters. Note the involvement of core and ligand sphere for all difference electron densities for the purely organic compounds, in marked contrast to the hybrids where four out of six cases only involve core atoms in the excitation process.

To investigate these differences experimentally and to study the effect of EWG and EDG bound to the substituents on the non-linear optical emission properties, we sought to synthesize the chosen compounds according to or similar to their reported syntheses. We have previously reported the emission spectrum of 4.^[6b] Compounds 2, 3, and 5 were obtained as amorphous powders by modifying previously reported reactions, i.e., using (TMS)₂S in toluene instead of Na₂S in acetone/H₂O,^[6b,15] but we were unable to synthesize the “extreme” species 1 and 6 despite multiple attempts.

The synthesis of Ad(*p*-CN-Ph)₄ (7) began with Ad(*p*-I-Ph)₄ utilizing the Rosenmund-von Braun reaction. To work up the reaction mixture, ethylenediamine was used in the literature to eliminate the nitrile-copper cyanide complexes and followed by nitrile extraction.^[16] However, ethylenediamine was inefficient in our case, but an excess of aqueous KCN was beneficial for the synthesis of 7. Our literature procedures were used to synthesize Ad(*m*-F-Ph)₄ (8) and Ad(*p*-F-Ph)₄ (9), yielding the desired products in good yields.^[17] AdPh₄ (10) can readily be synthesized and has been well studied.^[18] The synthetic routes

Table 1. Natural population partial charge (Q) analysis of (R-PhSn)₄S₆ and Ad(R-Ph)₄. Q_{Core} is defined for all Sn and S atoms for 1–6 and all C and H in the adamantane core for 7–12, Q_{RPh} is defined as all atoms that are not part of Q_{Core}.

Group R	<i>p</i> -CN	<i>m</i> -F	<i>p</i> -F	H	<i>p</i> -OMe	<i>p</i> -NMe ₂
Hammett σ	+0.66	+0.34	+0.06	0.00	–0.27	–0.83
Compound	1	2	3	4	5	6
Total Q _{Core}	+1.48	+1.46	+1.45	+1.43	+1.42	+1.39
Total Q _{RPh}	–1.48	–1.46	–1.45	–1.43	–1.42	–1.39
Compound	7	8	9	10	11	12
Total Q _{Core}	+0.01	0.00	0.00	0.00	–0.01	–0.02
Total Q _{RPh}	–0.01	0.00	0.00	+0.01	+0.01	+0.02

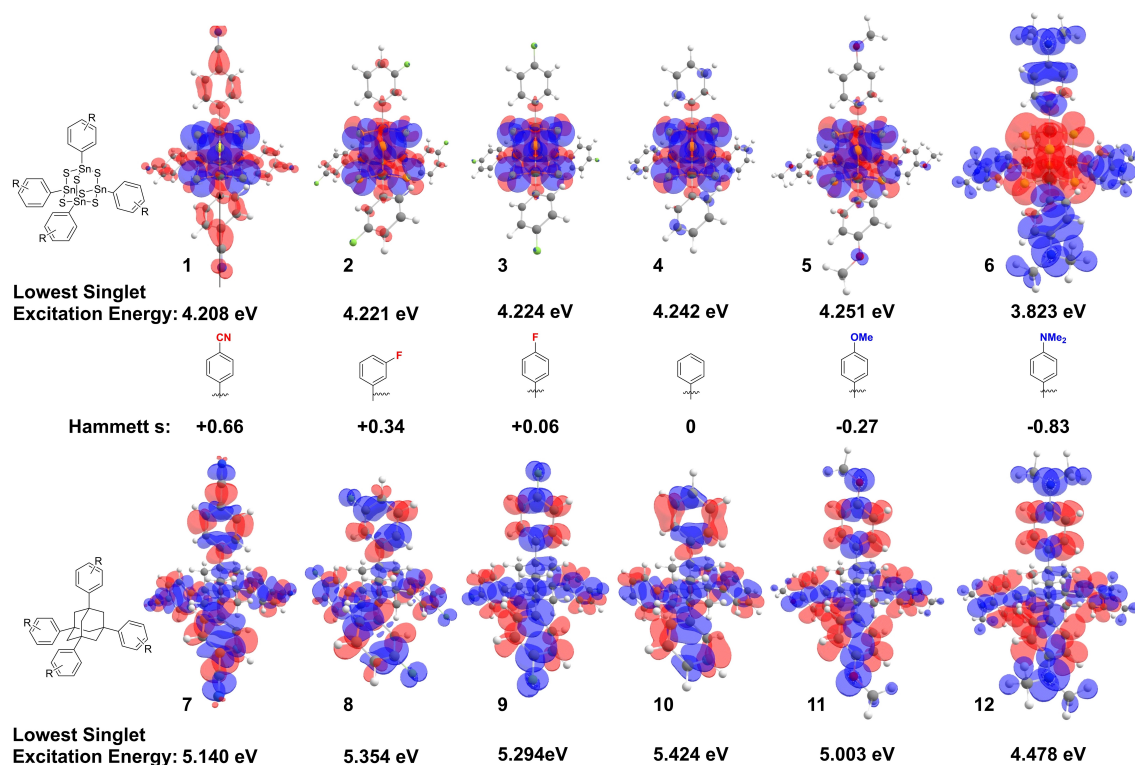
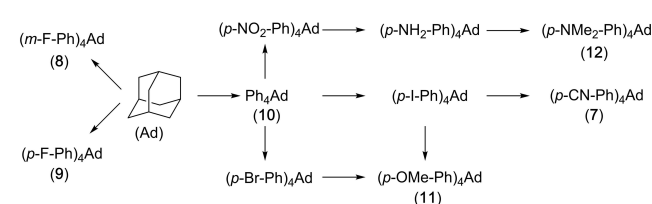


Figure 1. Difference electron densities and the associated excitation energies for the first singlet adiabatic excitation event for $[(R\text{-PhSn})_4S_6]$ (compounds 1–6; top) and $Ad(R\text{-Ph})_4$ (compounds 7–12; bottom), computed with TD-DFT at PBE0/def2-TZVP. Contours were plotted at 0.0005 a.u. Blue contours indicate an excess of electron density in the ground state while red contours indicate an excess of electron density in the excited state (excitations “from blue to red”).

to 11 were adopted from the literature with slight modifications.^[19] The iodination of 10 with $Ph(OCOCF_3)_2$ in chloroform solution of iodine gives $Ad(p\text{-I-Ph})_4$. The reaction of $Ad(p\text{-I-Ph})_4$ with NaOMe and Cu(I)Br in dry MeOH/DMF yields 11. The reaction of $Ad(p\text{-Br-Ph})_4$ with NaOMe and Cu(I)Br in dry MeOH/DMF yields 11 with a mixture of side products.^[20] We attempted to synthesize 12 by nitration of 10 to produce $Ad(p\text{-NO}_2\text{-Ph})_4$ which could be reduced to produce $Ad(p\text{-NH}_2\text{-Ph})_4$ and subsequently methylated to afford the target product 12 (Scheme 2).^[21] However, this synthetic pathway proved unsuccessful.^[22] Compounds 8, 9, and 11 were obtained as crystalline solids while 7 and 10 were powders; 7–11 were characterized by 1H NMR spectroscopy. The crystal structures of 8–11 were reported before, while that of 7 was not. Crystals of 7 suitable for X-ray diffraction analysis were obtained by dissolving 7 in toluene, refluxing it at $110^\circ C$ overnight and slow cooling (Table S1 and Figure S20).



Scheme 2. Synthetic access to tetraaryl substituted adamantane derivatives.

We set out to analyze the non-linear optical responses of 2, 3, 5, and 7–11. We previously demonstrated that irradiating pulverized 4 and 10 with a continuous wave (CW) laser produces a white-light continuum.^[6c,17] As illustrated in Figure 2a, compounds 2, 3, and 5 produced white light when exposed to 980 nm CW-laser irradiation (728 mW). Compound 5 produces a slightly red-shifted spectrum ($\Delta\lambda_{\text{max}} \approx 20$ nm) relative to 2 and 3, which correlates with the described changes in the electronic structure when the functional groups become more electron-donating (irrespective of the nearly unaffected excitation wavelength). Note that beside WLG, irradiation can cause decomposition of the samples if done with too high a laser power (Figure S32); the applied laser power was thus carefully tuned (see also below). As we also recognized that the

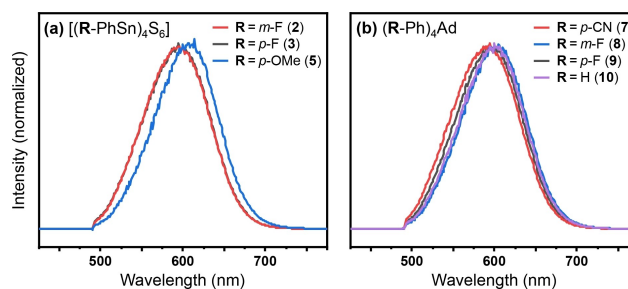


Figure 2. Photopic white-light spectra of compounds 2, 3, and 5 (a), and of compounds 7–10 after ball milling. All spectra were obtained upon irradiation with a 980 nm laser at a power output of 728 mW.

compounds tend to melt under the measurement conditions, we hypothesize that the emitting materials can be generated *in situ* even from crystalline material, as previously reported.

The effect of different morphologies was studied on the organic adamantane derivatives. We used a ball mill for pulverizing compounds 7–11, which served to turn them into fine powders with partial amorphicity. This process is not quantitative though; even after long ball-milling times (16 h) some crystallinity was still evident as proven by PXRD analyses (see Figures S15–S19). However, the amount of amorphous material in the ball-milled samples of 7–10 apparently sufficed for WLG (Figure 2b). Again, *in situ* amorphization by melting under irradiation is supposed to contribute to WLG. In contrast to the inorganic analogs [(R-PhSn)₄S₆], compounds 7–10 did not show signs of decomposition (Figure S33), indicating that these samples are more stable than their inorganic cousins. In agreement with the observation that there are no notable changes in the electronic structures of the organic clusters along the Hammett series, the shifts in maximum wavelengths are even smaller than for the inorganic clusters ($\Delta\lambda_{\text{max}} < 10$ nm).

To our surprise, ball-milled 11 did not produce any visible response. First, we hypothesized that residual crystallinity in the ball-milled sample 11 prevented WLG entirely (Figure 3a, blue line). Therefore, we converted 11 completely into a perfectly amorphous form by hot-melt quenching (Figure 3a, red line). However, neither highly crystalline nor amorphous 11 emits white light (Figure 3b; the shown signal represents the fundamental laser line). Hence, the –OMe substituent, which also displays the lowest Hammett σ value, significantly diminishes the nonlinear optical response. The obvious contradiction to the observation of WLG by compound 5 suggested that we need to look for yet another reason for the phenomenon to occur.

We therefore investigated the effect of the applied laser power on the resulting emission spectra, which we exemplify for compound 7 first. As the laser power was reduced from 728 mW to 50 mW, the intensity of the emission spectrum of 7 decreased (Figure 4a,b). No WLG was observed when the laser power was reduced below 50 mW. These results suggest that strong EWGs on organic adamantane derivatives such as –CN

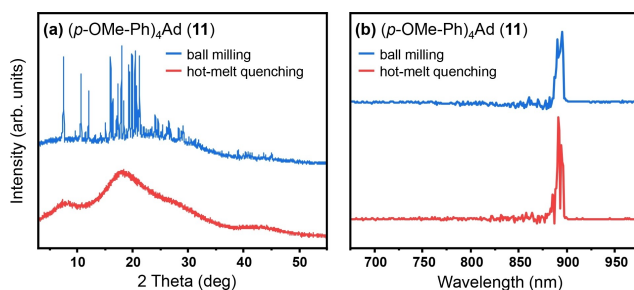


Figure 3. Powder X-ray diffraction patterns (a) and study of the optical responses (b) of compound 11 after ball milling (blue lines) and hot-melt quenching (red lines). The optical measurements shown in (b) were done with an irradiation wavelength of 980 nm at a power output of 728 mW; the signals represents the remaining (therefore magnified and noisy) cut-off of the fundamental laser line, as obtained using the short pass filter (Thorlabs FESH900) to attenuate the fundamental line.

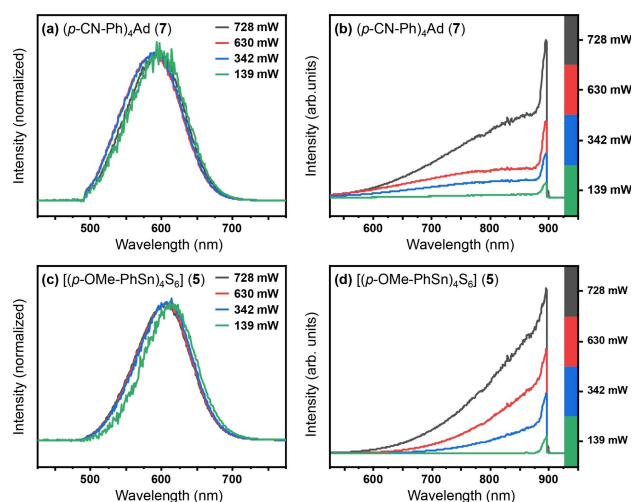


Figure 4. (a) Photopic white-light spectra of compound 7 upon irradiation with a 980 nm laser at various pumping powers. (b) Radiometric spectra for additional illustration of the effect; note that the intensities are also arbitrary in this graphic, but their changing shape reflects the observed increase of intensity. (c) Photopic white-light spectra of 5 upon irradiation with a 980 nm laser at various pumping powers. (d) Radiometric spectra without normalization for additional illustration of the effect; note that the intensities are arbitrary and clearly reflect the mere extension of the intensity axis for representation (i. e., no intensity increase).

allow for lower pumping powers to effectively cause WLG. By comparison, a power of 630 mW was required for 8 and 9 (Figures S27 and S28), so EDGs accordingly increase the minimum required pumping power for these compounds. This explains the lack of response for 11, which does not produce intensities even above 728 mW.

In comparison, no such trend was observed for compounds 2, 3, and 5, which require a minimum laser power of 342 mW, 630 mW, and 139 mW, respectively, to generate WLG (see Figure 4c,d for compound 5, Figure S30 for compound 2, and Figure S31 for compound 3).

Again, we see a clear difference between inorganic [(R-PhSn)₄S₆] clusters and organic adamantane derivatives Ad(R-Ph)₄ from these experiments, which, in summary, allow the following conclusions: (a) Hammett values of the functional groups R on the phenyl ligands of inorganic clusters notably affect the electronic structure and also the excitation event and (slightly) the maximum emission wavelength, while a correlation between σ and the required laser pumping power is not visible. (b) For organic adamantane derivatives, the situation is inverse, with the Hammett values of R not affecting the excitation process, nor notably affecting the maximum WLG emission wavelength, but having a strong effect on the minimum pumping power of the laser required to produce WLG. The latter goes so far as to completely inhibit WLG (or any other non-linear response) to occur for Ad(p-MeO-Ph)₄ bearing the strongest electron-donating groups studied herein. Based on these results, it can be generally stated that, on the one hand, the energetic features of the excitation events are only weakly correlated with the resulting white-light emission process and that, on the other hand, the most important impact that electronically different substituents can have on

the WLJ process (beside their effect on phase transition properties of the compounds) concerns the laser power needed to observe WLJ at all. We therefore need to discuss statistical aspects of the emission in the future in more detail, which brings us an important step towards understanding this still unraveled physical process.

Experimental Section

Details regarding experimental procedures, full compound characterization, crystal structure analyses, and computational methods can be found in the Supporting Information. The xyz coordinates of all optimized structures are available as separate documents (ascii format). Deposition Number 2124083 (for **7**) contains the supplementary crystallographic data for this paper. These data are provided free of charge by the joint Cambridge Crystallographic Data Centre and Fachinformationszentrum Karlsruhe Access Structures service.

Acknowledgments

This work was financially supported by the Deutsche Forschungsgemeinschaft (FOR 2824). The authors wish to thank Dr. Nils W. Rosemann (KIT) for his expert help with the WLJ measurement of $Ad(p-F-Ph)_4$ and $[(p-F-PhSn)_4S_6]$, and Dr. Jonathan Becker for his help with the X-ray structural analyses. Open Access funding enabled and organized by Projekt DEAL.

Conflict of Interest

The authors declare no conflict of interest.

Data Availability Statement

The data that support the findings of this study are available in the supplementary material of this article.

Keywords: adamantane derivatives · DFT computations · organotininsulfide clusters · substituent effects · supercontinuum generation

- [1] a) C. Chen, J. Wang, *Analyst* **2020**, *145*, 1605–1628; b) N. Khansili, G. Rattu, P. M. Krishna, *Sens. Actuators B* **2018**, *265*, 35–49; c) J. Galbán, V. Sanz, E. Mateos, I. Sanz-Vicente, A. Delgado-Camín, S. de Marcos, *Protein Pept. Lett.* **2008**, *15*, 772–778; d) J. Park, J.-M. Lee, H. Chun, Y. Lee, S. J.

- Hong, H. Jung, Y.-J. Kim, W.-G. Kim, V. Devaraj, E. J. Choi, J.-W. Oh, B. Han, *Biosens. Bioelectron.* **2021**, *177*, 112979.
 [2] a) B. D. Ravetz, A. B. Pun, E. M. Churchill, D. N. Congreve, T. Rovis, L. M. Campos, *Nature* **2019**, *565*, 343–346; b) L. Huang, W. Wu, Y. Li, K. Huang, L. Zeng, W. Lin, G. Han, *J. Am. Chem. Soc.* **2020**, *142*, 18460–18470.
 [3] a) C. Y. Li, B. Wei, Z. K. Hua, H. Zhang, X. F. Li, J. H. Zhang, in *2008 58th Electronic Components and Technology Conference*, **2008**, pp. 1819–1824; b) A. J. Steckl, J. Heikenfeld, S. C. Allen, *J. Disp. Technol.* **2005**, *1*, 157; c) M. Mosca, R. Macaluso, I. Crupi, in *Polymers for Light-Emitting Devices and Displays*, **2020**, pp. 197–262; d) T. Sekitani, H. Nakajima, H. Maeda, T. Fukushima, T. Aida, K. Hata, T. Someya, *Nat. Mater.* **2009**, *8*, 494–499; e) Y. Gao, C. Huang, C. Hao, S. Sun, L. Zhang, C. Zhang, Z. Duan, K. Wang, Z. Jin, N. Zhang, A. V. Kildishev, C.-W. Qiu, Q. Song, S. Xiao, *ACS Nano* **2018**, *12*, 8847–8854.
 [4] Y. I. Park, K. T. Lee, Y. D. Suh, T. Hyeon, *Chem. Soc. Rev.* **2015**, *44*, 1302–1317.
 [5] a) S. Pimpurkar, J. S. Speck, S. P. DenBaars, S. Nakamura, *Nat. Photonics* **2009**, *3*, 180–182; b) J. Cho, J. H. Park, J. K. Kim, E. F. Schubert, *Laser Photonics Rev.* **2017**, *11*, 1600147.
 [6] a) N. W. Rosemann, J. P. Eußner, A. Beyer, S. W. Koch, K. Volz, S. Dehnen, S. Chatterjee, *Science* **2016**, *352*, 1301–1304; b) N. W. Rosemann, J. P. Eußner, E. Dornsiepen, S. Chatterjee, S. Dehnen, *J. Am. Chem. Soc.* **2016**, *138*, 16224–16227; c) N. W. Rosemann, H. Locke, P. R. Schreiner, S. Chatterjee, *Adv. Opt. Mater.* **2018**, *6*, 1701162; d) I. Rojas-León, J. Christmann, S. Schwan, F. Ziese, S. Sanna, D. Mollenhauer, N. W. Rosemann, S. Dehnen, *Adv. Mater.* **2022**, *34*, 2203351.
 [7] E. Dornsiepen, F. Dobener, S. Chatterjee, S. Dehnen, *Angew. Chem. Int. Ed.* **2019**, *58*, 17041–17046; *Angew. Chem.* **2019**, *131*, 17197–17202.
 [8] a) M. Louzada, J. Britton, T. Nyokong, S. Khene, *J. Phys. Chem. A* **2017**, *121*, 7165–7175; b) P. G. Lacroix, I. Malfant, C. Lepetit, *Coord. Chem. Rev.* **2016**, *308*, 381–394.
 [9] In TURBOMOLE Version 7.5, TURBOMOLE GmbH 2018. TURBOMOLE is a development of University of Karlsruhe and Forschungszentrum Karlsruhe 1989–2007, TURBOMOLE GmbH since 2007.
 [10] E. D. Glendenning, C. R. Landis, F. Weinhold, *WIREs Comput. Mol. Sci.* **2012**, *2*, 1–42.
 [11] C. Hansch, A. Leo, R. W. Taft, *Chem. Rev.* **1991**, *91*, 165–195.
 [12] F. Weigend, R. Ahlrichs, *Phys. Chem. Chem. Phys.* **2005**, *7*, 3297–3305.
 [13] B. Metz, H. Stoll, M. Dolg, *J. Chem. Phys.* **2000**, *113*, 2563–2569.
 [14] J. P. Perdew, K. Burke, M. Ernzerhof, *Phys. Rev. Lett.* **1996**, *77*, 3865–3868.
 [15] H. Berwe, A. Haas, *Chem. Ber.* **1987**, *120*, 1175–1182.
 [16] a) T. Mocanu, L. Pop, N. D. Hädade, S. Shova, L. Sorace, I. Grosu, M. Andruh, *Eur. J. Inorg. Chem.* **2019**, *2019*, 5025–5038; b) I. Boldog, K. V. Domasevitch, I. A. Baburin, H. Ott, B. Gil-Hernández, J. Sanchiz, C. Janiak, *CrystEngComm* **2013**, *15*, 1235–1243.
 [17] S. Gowrisankar, B. Bernhardt, J. Becker, P. R. Schreiner, *Eur. J. Org. Chem.* **2021**, *48*, 6806–6810.
 [18] H. Newman, *Synthesis* **1972**, 692–693.
 [19] A. Schwenger, W. Frey, C. Richert, *Chem. Eur. J.* **2015**, *21*, 8781–8789.
 [20] C. Shen, H. Yu, Z. Wang, *Chem. Commun.* **2014**, *50*, 11238–11241.
 [21] S. Zulfiqar, D. Mantione, O. El Tall, M. I. Sarwar, F. Ruipérez, A. Rothenberger, D. Mecerreyes, *J. Mater. Chem. A* **2016**, *4*, 8190–8197.
 [22] X.-D. Li, S.-Q. Feng, F. Guo, X.-Y. Liu, J.-X. Yu, Z.-W. Hou, *RSC Adv.* **2016**, *6*, 21517–21525.

Manuscript received: May 19, 2022
 Revised manuscript received: July 23, 2022
 Accepted manuscript online: July 25, 2022
 Version of record online: August 22, 2022